Metastable lifetimes in a kinetic Ising model: Dependence on field and system size

Per Arne Rikvold,[1,2,3,*] H. Tomita,[1] S. Miyashita,[2] and Scott W. Sides[3]
[1] *Department of Fundamental Sciences, Faculty of Integrated Human Studies, Kyoto University, Kyoto 606, Japan*
[2] *Graduate School of Human and Environmental Studies, Kyoto University, Kyoto 606, Japan*
[3] *Supercomputer Computations Research Institute, Center for Materials Research and Technology, and Department of Physics, Florida State University, Tallahassee, Florida 32306-4052*
(Received 26 January 1994)

The lifetimes of metastable states in kinetic Ising ferromagnets are studied by droplet theory and Monte Carlo simulation, in order to determine their dependences on applied field and system size. For a wide range of fields, the dominant field dependence is universal for local dynamics and has the form of an exponential in the inverse field, modified by universal and nonuniversal multiplicative power-law prefactors. Quantitative droplet-theory predictions for these dependences are numerically verified, and small deviations from the predictions are shown to depend nonuniversally on the details of the dynamics. We identify four distinct field intervals in which the field dependence and statistical properties of the lifetimes are markedly different. The field marking the crossover between the weak-field regime, in which the decay is dominated by a single droplet, and the intermediate-field regime, in which it is dominated by a finite density of droplets, vanishes logarithmically with system size. As a consequence, the slow decay characteristic of the former regime may be observable in systems that are macroscopic as far as their equilibrium properties are concerned.

PACS number(s): 64.60.My, 64.60.Qb, 05.70.Ln, 05.50.+q

I. INTRODUCTION

Although it is observed in nature in contexts as dissimilar as supercooled water or water vapor [1–3] and the electroweak [4] and QCD confinement-deconfinement [5] phase transitions, metastability is very difficult to characterize in a microscopically precise fashion [6]. In certain systems with weak long-range interactions infinitely long-lived metastable states can exist in the thermodynamic limit [7], and metastability in such systems has been studied with several techniques [8], including field-theoretical, Monte Carlo (MC), and transfer-matrix methods. However, in systems with short-range interactions metastable states eventually decay, even though their lifetimes may be many orders of magnitude larger than other characteristic time scales of the system and may even become comparable to the age of the universe [1]. In order to gain a deeper understanding of metastability in short-range systems, it is necessary to consider in detail the lifetimes of metastable states and how they are determined by the physical mechanisms involved in the decay [9].

As a prototype for the metastable dynamics of short-range systems, the decay of the magnetization in impurity-free kinetic Ising ferromagnets in unfavorable applied fields has been studied by MC methods in both two [10–18] and three [19–21] dimensions. The results of several of these studies were analyzed in terms of droplet theory [22–28], establishing general agreement between theory and simulations. In the present work we further investigate the extent of that agreement by analytical droplet-theory calculations and MC simulations. We emphasize the dependences on applied field and system size of the metastable lifetimes and their relations to particular decay mechanisms. Our analysis extends a recent study by two of us [29,30], and Ref. [29] is henceforth referred to as I.

The main results in I can be summarized as follows. In agreement with previous [14,20] and more recent [21] simulations it was found that the statistical properties and system-size dependence of the metastable lifetimes in MC simulations were markedly different in two separate field regions. The point separating these regions was called "the dynamic spinodal point" (DSP), and the corresponding field, which depends on temperature and system size, was denoted $H_{\rm DSP}$. For $|H| > H_{\rm DSP}$, the mean lifetime was observed to be independent of system size and much greater than its standard deviation [14,20,21]. This field region was therefore called "the deterministic region." For weaker fields, the mean lifetime was inversely proportional to the system volume [14,15,20,21,23–25] and the standard deviation was approximately equal to the mean [14,20,21]. For these reasons this regime was termed "the stochastic region." The position of the DSP, which separates these regions, depends on the temperature and system size. The main goal of the present work is to understand and quantify these dependences.

In this paper we present a quantitative analysis of metastable lifetimes in terms of a droplet model of homogeneous nucleation in d-dimensional systems [22–28], obtaining analytic results for the logarithmic derivative of the lifetime with respect to $1/|H|^{d-1}$, as well as the explicit size and temperature dependence of $H_{\rm DSP}$. Both

*Permanent address: Supercomputer Computations Research Institute, Center for Materials Research and Technology, and Department of Physics, Florida State University, Tallahassee, FL 32306-4052. Electronic address: rikvold@scri.fsu.edu

the deterministic and the stochastic regions are found to be divided into two subregions, and expressions for the corresponding crossover fields are derived. These analytic results are shown to be in excellent agreement with MC simulations for $d=2$ at a temperature of $0.8T_c$.

In order of increasingly strong unfavorable field the distinct regions that we identify are the "coexistence region," characterized by subcritical fluctuations on the scale of the system volume; the "single-droplet region," characterized by decay via a single critical droplet; the "multidroplet region," characterized by decay via a finite density of droplets; and the "strong-field region," in which the droplet picture is inappropriate. The two former regions comprise the stochastic region, and the two latter ones the deterministic region. The DSP thus marks the crossover between the single-droplet and multidroplet regions. The crossover between the coexistence region and the single-droplet region was called "the thermodynamic spinodal point" (THSP) in I, and the crossover between the strong-field and multidroplet regions was called "the mean-field spinodal point" (MFSP). These different regions and the crossover points that separate them are summarized in Fig. 1, which shows a schematic sketch of the field dependence of the average metastable lifetime.

Whereas the dominant field dependence of the lifetime in the single-droplet and multidroplet regions is exponential in the inverse field, our MC data are sufficiently precise to also allow evaluation of multiplicative power-law prefactors. These are predicted by droplet theory [23–27], but are difficult to detect numerically and, to our knowledge, have not previously been measured in MC studies of lifetimes or nucleation rates.

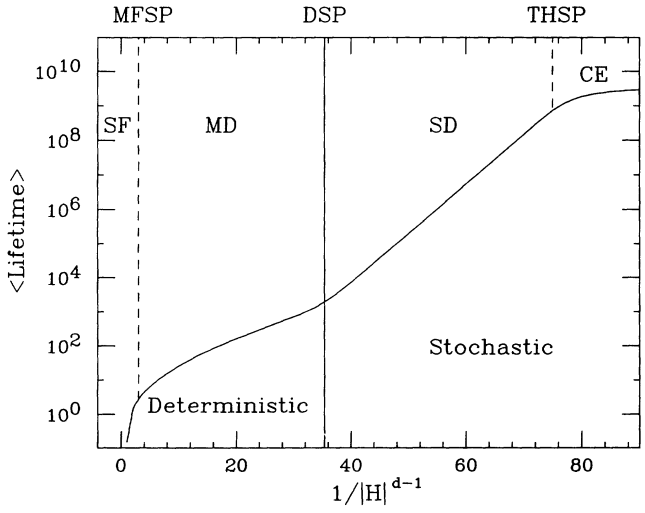

FIG. 1. Schematic sketch showing the field dependence of the average metastable lifetime for a d-dimensional kinetic Ising model on a logarithmic scale. The dynamic spinodal point is indicated by the solid vertical line labeled DSP. To its left is the deterministic region and to its right is the stochastic region. The deterministic region is divided into the strong-field (SF) and multidroplet (MD) subregions by the mean-field spinodal, indicated by the dashed vertical line labeled MFSP. The stochastic region is divided into the single-droplet (SD) and coexistence (CE) subregions by the thermodynamic spinodal, indicated by the dashed vertical line labeled THSP. This figure is based on the analytical and numerical results presented in this paper, but it is not drawn to scale for a specific system size. In particular, the extent of the single-droplet region is greatly reduced, relative to the multidroplet region.

The rest of the paper is organized as follows. In Sec. II the kinetic Ising model is defined and the numerical methods used in this work are discussed. In Sec. III the droplet-theoretical predictions are developed for both infinitely large and finite systems. In Sec. IV the numerical results are presented and compared with the theory, and Sec. V contains a brief discussion.

II. MODEL AND NUMERICAL METHODS

The model is defined by the reduced Hamiltonian

$$\mathcal{H}/k_BT = -K\sum_{\langle i,j\rangle} s_i s_j - H\sum_i s_i \,, \tag{1}$$

where $s_i = \pm 1$ is the spin at site i, T is the temperature, k_B is Boltzmann's constant, and $K = J/k_BT$ (>0), and $H = h/k_BT$ are the reduced coupling constant and field, respectively. The sums $\sum_{\langle i,j\rangle}$ and $\sum_i$ run over all nearest-neighbor (NN) pairs and over all N sites on a d-dimensional hypercubic lattice, respectively.

The dynamics is given by the Metropolis single-spin-flip MC algorithm. The transition probability for a flip of the spin at site α from s_α to $-s_\alpha$ is thus defined as [31]

$$W(s_\alpha \to -s_\alpha) = \min[1, \exp(-\Delta E_\alpha)] \,, \tag{2a}$$

where

$$\Delta E_\alpha = 2s_\alpha\left[K\sum_{\mathrm{NN}} s_\beta + H\right] \tag{2b}$$

with sum over the NN sites surrounding α is the energy change during the flip, divided by k_BT.

We study the relaxation of the magnetization

$$m(t) = N^{-1}\sum_{i=1}^{N} s_i(t) \,, \tag{3}$$

starting from an initial state magnetized opposite to the applied field. This approach was also used, e.g., in Ref. [21]. The magnetization $m(t)$ is directly obtained as an average over the droplet size distribution [18,21,22] and it is closely related to the nonequilibrium relaxation functions introduced by Binder [11]. The volume fraction of stable phase at time t is $\phi_s(t) = [m_{\mathrm{ms}} - m(t)]/[m_{\mathrm{ms}} - m_s]$, where m_s and m_{ms} are the bulk equilibrium and metastable magnetizations, respectively.

The simulations were performed on square $L\times L$ systems, with L=64, 128, 256, 400, and 720 and periodic boundary conditions. The systems were initialized with $m(0)=+1$ and allowed to develop in a constant field $H<0$ at $T=0.8T_c$ ($K=0.550\,858...$). This temperature is high enough to obtain reasonable MC acceptance rates, but it is sufficiently low to avoid complications such as critical slowing-down and possible finite-size scaling effects due

to small droplets [32]. For later reference we note that the equilibrium magnetization at $0.8T_c$ is $m_s = 0.954\,410...$ [33] and the equilibrium surface tension along a primitive lattice vector is $\sigma_0 = 0.745\,915...$ [34].

Average first-passage times to m=0.9, 0.8, ..., 0.0 were recorded, together with their empirical standard deviations, and the mean lifetime of the metastable state was estimated as the average first-passage time to m=0.7. We used this particular cutoff magnetization for the following reasons. In order for the droplet-theoretical considerations developed in Sec. III to remain valid during the whole time evolution until the cutoff, the cutoff value of ϕ_s should be below the percolation limit. However, the cutoff magnetization should not be so close to m_{ms} that subcritical fluctuations in the metastable phase ("recrossing events" [16]) might be mistaken for decay events, thus leading to significant underestimation of the mean lifetime. The cutoff magnetization m=0.7, which, assuming $m_{ms} = -m_s$, corresponds to $\phi_s \approx 0.13$, was chosen as a reasonable compromise. However, except for very strong and very weak fields, the dependence of the observed lifetimes on the cutoff is weak, and results almost identical to those reported here were obtained with cutoff at m=0.0, or $\phi_s \approx 0.5$.

A more accurate, but also more computationally intensive, method to estimate the lifetimes would be to use the recrossing events by choosing as a field-dependent cutoff a value of m which lies on the side of the maximum of the recrossing-event distribution [16] opposite from that of the initial magnetization, and for which the recrossing-event probability is below a given threshold. We do not implement this method here, but plan to do so in future studies.

For fields at which the lifetime is large, the magnetization $m(t)$ was measured after each MC step per site (MCS), whereas for shorter lifetimes it was measured after each successful spin flip. The latter method was used whenever necessary in order to ensure that the uncertainty due to the discreteness of the time variable was at least one order of magnitude smaller than the standard deviations in the average first-passage times.

The numerical data were obtained with a special-purpose m-TIS2 computer [35,36] at Kyoto University and on heterogeneous clusters of IBM RS/6000, DECstation, and DEC 3000 Model 400 Alpha workstations at Florida State University.

The m-TIS2 architecture only allows the MC updates to be performed sequentially, and the available memory limited the maximum system size to L=720. To assess the effects of the former restriction, simulations with updates at randomly chosen sites were performed on the workstation clusters for L=128 and 720. The total computer time spent was approximately 400 m-TIS2 hours and 1600 hours of workstation time for the sequential-update study, and an additional 13 000 workstation hours for the random-update investigation.

III. DROPLET THEORY

In this section we derive the droplet-theoretical relations necessary to interpret the simulated lifetime data.

The system is characterized by six length scales: the lattice constant, which we take as unity; the single-phase correlation lengths in the stable and metastable phases, ξ_s and ξ_{ms}, respectively; the critical droplet radius R_c; the size R_0 to which one droplet can grow before it is likely to meet another, which we shall refer to as the mean droplet separation; and the system size L. Here we only consider cases in which ξ_s is smaller than the other length scales, i.e., well below the critical temperature. Thus we are left to consider the interplay between four lengths: L, R_0, R_c, and ξ_{ms}.

A. Infinite systems

First we obtain R_0 and R_c for d-dimensional systems in the limit $L \to \infty$. Although the droplets are almost circular at our simulation temperature, we give a general argument that remains valid for low temperatures, at which nonspherical droplets appear because of the anisotropy of the surface tension [34,37–41]. The free energy of a (regular, but not necessarily spherical) d-dimensional droplet of radius R (defined as half the extent of the droplet along a primitive lattice vector) and volume $V(R) = \Omega_d R^d$ is

$$\begin{aligned} F(R) &= V^{(d-1)/d}\widehat{\Sigma} - V\Delta \\ &= \Omega_d^{(d-1)/d} R^{d-1}\widehat{\Sigma} - \Omega_d R^d \Delta \,, \end{aligned} \tag{4}$$

where Δ is the difference in bulk free-energy density between the metastable and stable states. The quantity $\widehat{\Sigma}$ is a temperature- and, in principle, field-dependent proportionality factor which relates the surface contribution to $F(R)$ with the droplet volume [34,42]. Applying standard droplet-theory arguments [27] to $F(R)$, one finds the critical radius, the free-energy cost of a critical droplet, and the nucleation rate per unit time and volume. The critical radius is

$$R_c(T,H) = \frac{(d-1)}{\Delta}\frac{\widehat{\Sigma}}{d\Omega_d^{1/d}} = \frac{(d-1)\sigma_0}{\Delta} \approx \frac{(d-1)\sigma_0}{2m_s k_B T|H|} \,, \tag{5}$$

where $\sigma_0 = \widehat{\Sigma}/(d\Omega_d^{1/d})$ is the surface tension along a primitive lattice vector [34]. The approximation $\Delta \approx 2m_s k_B T|H|$, where $m_s(T)$ is the spontaneous equilibrium magnetization, is expected to be valid not only at low temperatures, but even near the critical point [39]. The free-energy cost of a critical droplet is

$$\begin{aligned} F_c(T,H) &= \left(\frac{d-1}{\Delta}\right)^{d-1}\left(\frac{\widehat{\Sigma}}{d}\right)^d \\ &\approx \left(\frac{d-1}{2m_s k_B T|H|}\right)^{d-1}\left(\frac{\widehat{\Sigma}}{d}\right)^d \,, \end{aligned} \tag{6}$$

and the nucleation rate per unit time and volume $I(T,H)$ is determined by F_c through [23–26]

$$I(T,H) = A(T)|H|^{b+c} e^{-\frac{F_c(T,H)}{k_B T}} \approx A(T)|H|^{b+c} e^{-\frac{\Xi}{|H|^{d-1}}} \tag{7a}$$

with

$$\Xi = \left(\frac{d-1}{2m_s}\right)^{d-1} \left(\frac{\widehat{\Sigma}}{dk_BT}\right)^{d} , \tag{7b}$$

where the approximation introduced in the second part of Eq. (7a) is the same as in Eqs. (5) and (6). The function $A(T)$ is expected to be nonuniversal, b is a universal exponent related to Goldstone-mode "wobbles" on the droplet surfaces [23,26], and c gives the H dependence of the "kinetic prefactor" [24,25], which is the only part of $I(T,H)$ that may depend explicitly on the specific dynamics. A field-theoretical calculation gives [26]

$$b = \begin{cases} (3-d)d/2 & \text{for } 1<d<5,\ d\neq 3 \\ -7/3 & \text{for } d=3. \end{cases} \tag{8}$$

Strictly speaking, a multiplicative correction term of form $[1+O(H^2)]$ should be included in the exponent in Eq. (7a) [26,39–41,43,44], but its effect on the metastable lifetimes is small for the relatively weak fields on which we focus our attention in this work, and it has therefore been suppressed for simplicity.

For $d=2$ there is substantial numerical evidence that $b=1$, as predicted by Eq. (8). This is obtained from calculations that do not involve the dynamics, such as analyses of series expansions [39,45,46] and transfer-matrix calculations [40,41]. These studies, as well as MC work [43,44], also indicate that the free-energy cost of the critical droplet is given by Eq. (6) with the zero-field equilibrium value for $\widehat{\Sigma}$. We therefore adopt the notations $\widehat{\Sigma}(T)$ and $\Xi(T)$ to emphasize the lack of field dependence in these quantities. They can be obtained with arbitrary numerical precision by combining a Wulff construction with the exact, anisotropic zero-field surface tension [34]. This general result, that the surface free energy of compact critical droplets is determined by the zero-field equilibrium surface tension, is also supported by MC studies of nucleation rates in three dimensions [19–21]. For dynamics that can be described by a Fokker-Planck equation it is expected that the kinetic prefactor is proportional to R_c^{-2} [24–26], which by Eq. (5) would yield $c=2$. However, we are not aware that independent, numerical verifications of this result have been performed previously. As discussed in Sec. IV we find that the measured value of c depends on the MC update scheme.

Assuming that the growing droplets are not substantially deformed [47], the radial growth velocity is obtained in an Allen-Cahn approximation [27,48,49] as

$$v_\perp = (d-1)\Gamma\left(R_c^{-1}-R^{-1}\right) \overset{R\to\infty}{\longrightarrow} (d-1)\Gamma R_c^{-1} \equiv v_0 , \tag{9}$$

where Γ depends on the details of the kinetics. The mean droplet separation R_0 and its associated time scale t_0 are obtained from $v_\perp$ and the nucleation rate I by requiring that $R_0 = v_\perp t_0$ and $R_0^d t_0 I = 1$ [49]. If $R_0 \gg R_c$, so that $v_\perp \approx v_0$, then by using $v_0 \propto |H|$ from Eqs. (5) and (9), one obtains

$$t_0(T,H) = (v_0^d I)^{-\frac{1}{d+1}} = B(T)|H|^{-\frac{b+c+d}{d+1}} e^{\frac{1}{d+1}\frac{\Xi(T)}{|H|^{d-1}}} \tag{10a}$$

and

$$R_0(T,H) = v_0 t_0 = C(T)|H|^{-\frac{b+c-1}{d+1}} e^{\frac{1}{d+1}\frac{\Xi(T)}{|H|^{d-1}}} . \tag{10b}$$

The coefficients B and C have the same nonuniversal status as A in Eq. (7a). Although $R_c \sim |H|^{-1} \to \infty$ as $|H|\to 0$, $R_c/R_0 \to 0$ in the same limit.

If one assumes that the positions of the (possibly overlapping) growing droplets are uncorrelated, the volume fraction of stable phase at time t becomes

$$\phi_s(t) = 1 - \exp\left[-\frac{\Omega_d}{d+1}\left(\frac{t}{t_0}\right)^{d+1}\right] , \tag{11}$$

which is known as Avrami's law [49–52]. From this it is seen that the average time taken to reach a specific ϕ_s is

$$\langle t(\phi_s)\rangle = t_0(T,H)\left[-\frac{d+1}{\Omega_d}\ln(1-\phi_s)\right]^{1/(d+1)} . \tag{12}$$

The "ideal-gas" approximation leading to Avrami's law is expected to hold when the total volume fraction of droplets is sufficiently small that droplet-droplet correlations can be ignored. The intermediate-field region, in which Eq. (12) holds, we call *the multidroplet region.* It corresponds to the picture of decay through continuously nucleating and growing droplets, first introduced by Kolmogorov, Johnson and Mehl, and Avrami over fifty years ago [49–52].

For stronger fields, a picture based on localized droplets no longer adequately describes the system, which in that case decays via long-wavelength, unstable modes reminiscent of spinodal decomposition [27]. The crossover field separating the multidroplet region from this *strong-field region* was termed "the mean-field spinodal" in I. It is located at a field $H_{\rm MFSP} < 4K$ [30,53,54]. We expect that $R_c < R_0$ for all $H < H_{\rm MFSP}$. A recent argument based on a transfer-matrix calculation indicates that the single-phase correlation length in the metastable phase is given by $\xi_{\rm ms} \approx T/(4J-2h)$ at low T [41]. A rough estimate for the field at which droplet theory breaks down can be obtained by requiring that $2R_c = \xi_{\rm ms}$. This yields $H_{\rm MFSP} < 2K$ and specifically $H_{\rm MFSP}(0.8T_c) \approx 0.3$ with the critical-droplet diameter $2R_c \approx 1$, independent of system size. The dynamics in the strong-field region beyond $H_{\rm MFSP}$ will not be discussed in detail here.

B. Finite-size effects

Next we study the effects produced by a finite system size L. For simplicity we consider hypercubic systems of volume L^d with periodic boundary conditions. Effects of heterogeneous nucleation at free boundaries are discussed in Ref. [55]. In the large-L limit,

$$L \gg R_0 \gg R_c , \tag{13}$$

we use an approximate argument by which the system is partitioned into $(L/R_0)^d \gg 1$ cells of volume R_0^d. Each cell decays from the metastable state to the equilibrium

state in an independent Poisson process of rate $R_0^d I = t_0^{-1}$. The volume fraction is then self-averaging, with $\langle t(\phi_s)\rangle$ approximately equal to the infinite-system result of Eq. (12), and the relative standard deviation is

$$r = \frac{\sqrt{\langle t(\phi_s)^2\rangle - \langle t(\phi_s)\rangle^2}}{\langle t(\phi_s)\rangle} \approx (R_0/L)^{\frac{d}{2}}\rho\,, \tag{14}$$

where $\rho \approx 1$ is the relative standard deviation of a single Poisson process. The regime characterized by $r \ll 1$ was termed "the deterministic region" in I. It is subdivided into the multidroplet and strong-field subregions discussed above.

For smaller L, so that

$$R_0 \gg L \gg R_c\,, \tag{15}$$

the random nucleation of a single critical droplet in a Poisson process of rate $L^d I$ is the rate-determining step. This is followed by rapid growth, until this droplet occupies the entire system after an additional time much shorter than the average waiting time before a second droplet nucleates. Therefore, in this case the characteristic lifetime is

$$\begin{aligned}\langle t(\phi_s)\rangle &\approx \left[L^d I(T,H)\right]^{-1} \\ &\approx L^{-d}[A(T)]^{-1}|H|^{-(b+c)}e^{\frac{\Xi(T)}{|H|^{d-1}}}\end{aligned} \tag{16}$$

with $r \approx 1$ and only a weak dependence on the threshold ϕ_s. This single-droplet region is part of "the stochastic region" observed in I.

The crossover between the deterministic and stochastic regimes is determined by the condition $L \propto R_0$. We identify the crossover field with the "dynamic spinodal point" introduced in I, and in the limit $H \to 0$ we explicitly obtain from Eq. (10b)

$$\begin{aligned}H_{DSP} = &\left(\frac{1}{d+1}\frac{\Xi(T)}{\ln L}\right)^{\frac{1}{d-1}} \\ &\times\left[1 + O\left(\frac{\ln(\ln L)}{\ln L}\right) + O\left(\frac{1}{\ln L}\right)\right]\,.\end{aligned} \tag{17}$$

We emphasize that, although H_{DSP} vanishes as $L \to \infty$, the approach to zero is exceedingly slow, especially for d=3 and larger. Therefore, H_{DSP} may well be measurably different from zero for systems that are definitely macroscopic as far as their equilibrium properties are concerned. (As an illustration, increasing L from 100 to 10^{10} for d=3 decreases the leading term in H_{DSP} only to approximately one-half of its original value.) Recent exact results [53,54] indicate that if the limit $T \to 0$ is taken *before* $L \to \infty$, then H_{DSP} should remain nonzero. An estimate for the mean lifetime at H_{DSP} in the infinite-L limit is obtained by setting

$$\begin{aligned}\langle t \text{ at } H_{DSP}\rangle \propto t_0(T,H_{DSP}) &= \frac{R_0(T,H_{DSP})}{v_0(T,H_{DSP})} \\ &\propto L/H_{DSP} \sim L(\ln L)^{1/(d-1)}\,,\end{aligned} \tag{18}$$

where the nonuniversal temperature-dependent proportionality factors have been dropped.

Finally, we consider the limit

$$R_0 \gg R_c \gg L\,. \tag{19}$$

In this case the volume term can be neglected in Eq. (4), and the free-energy cost of a droplet occupying a volume fraction $\phi_s = V(R)/L^d$ is $F(\phi_s) = L^{d-1}\phi_s^{(d-1)/d}\widehat{\Sigma}(T)$, so that the first-passage time to a given ϕ_s is independent of H and diverges exponentially with L^{d-1}. Since the dynamics in this region of extremely weak fields or extremely small systems is similar to that on the coexistence line, H=0, we call it *the coexistence region.* The crossover field between the coexistence and single-droplet regions, called "the thermodynamic spinodal point" in I, is determined for a given ϕ_s by $\Omega_d(R_c/L)^d = \phi_s$, which yields

$$H_{THSP} = \frac{1}{L\phi_s^{1/d}}\frac{(d-1)\widehat{\Sigma}(T)}{2dk_BTm_s}\,. \tag{20}$$

IV. NUMERICAL RESULTS

The mean metastable lifetimes are illustrated in Fig. 2, which shows the average first-passage time to m=0.7 ($\phi_s \approx 0.13$) for two-dimensional square Ising systems with L=64,..., 720 at $0.8T_c$. The simulations were performed using the Metropolis single-spin-flip MC algorithm with sequential updates, as discussed in Sec. II. The lifetimes, in units of MCS, are plotted on a logarithmic scale vs $1/|H|$. Each data point is averaged over n=100 independent realizations, and the errors are calculated from the empirical standard deviation σ in $t(m$=0.7) as $\sigma/\sqrt{n}$. For given $|H|$ and sufficiently small L the lifetimes decrease with increasing L as $\langle t(\phi_s)\rangle \propto L^{-2}$, in agreement with Eq. (16) for the single-droplet region and as shown in Fig. 3 of I. For larger L they converge to an L-independent value, as expected from Eq. (12) for the multidroplet region. This L^{-d} behavior was previously remarked in Refs. [14,15,20,21], as was the presence of the L-independent regime in Refs. [14,20,21]. The size-independent data in the intermediate- and strong-field portions of Fig. 2 belong to the deterministic region, whereas the size-dependent data in the weak-field, long-time portion lie in the stochastic region. The droplet-theory results of Eqs. (10a), (12), and (16) show that in *both* the multidroplet and the single-droplet regions the field dependence of the lifetime is determined by the nucleation rate $I(T,H)$, so that the asymptotic slopes of $\ln\langle t(\phi_s)\rangle$ vs $1/|H|^{d-1}$ in the two regimes are related by a factor $(d+1)$. Based on the four points for L=64 in the single-droplet region of Fig. 2 ($1/|H| \geq 20$) the effective slope was estimated by a least-squares fit to be 0.36(1). This slope is indicated by the dashed line above the data in Fig. 2, whereas the dashed line below the data has 1/3 this slope. The agreement with droplet theory seems excellent. However, the measured effective slope is almost 30% larger than the theoretically predicted asymptotic slope, $\Xi(0.8T_c) = 0.278\,840...$, which is obtained by using the numerically exact [34,42] value $\widehat{\Sigma}(0.8T_c)/J = 2.648\,81...$ in Eq. (7b).

The explanation for this apparent discrepancy lies in the power-law prefactors in Eqs. (10a) and (16), which

yield the effective slopes

$$\Lambda_{\rm eff} \equiv \frac{d\ln\langle t(\phi_s)\rangle}{d(1/|H|^{d-1})} = \lambda|H|^{d-1} + \Lambda\,, \qquad (21)$$

with $\lambda=(b+c)/(d-1)$ and $\Lambda=\Xi(T)$ in the single-droplet region described by Eq. (16) and $\lambda=(b+c+d)/(d^2-1)$ and $\Lambda=\Xi(T)/(d+1)$ in the multidroplet region described by Eqs. (10a) and (12).

In Fig. 3 we show two-point finite-difference estimates for $\Lambda_{\rm eff}$, based on the average lifetimes in Fig. 2, for pairs of fields, $|H_1|>|H_2|$. These estimates are plotted vs the field value that occurs in the finite-difference version of Eq. (21), $|H|=|H_1H_2|\ln|H_1/H_2|/|H_1-H_2|$. The error bars are calculated as

$$\sigma_\Lambda = \sqrt{\left[\left(\frac{\sigma_1}{\langle t_1\rangle}\right)^2+\left(\frac{\sigma_2}{\langle t_2\rangle}\right)^2\right]\frac{1}{n}}\left|\frac{H_1H_2}{H_1-H_2}\right|\,,$$

where σ_i and $\langle t_i\rangle$ are the empirical standard deviation and mean for the lifetime at $|H_i|$, with $i=1$ or 2. For clarity only two system sizes, $L=128$ and 720, were included in the figure. The other sizes give results similar to those shown. The solid straight lines correspond to Eq. (21) with $b+c=2$ and the exact $\Xi(0.8T_c)=0.278\,840\ldots$. The data points for both system sizes cluster close to the lower of these two lines in the whole multidroplet region. However, in the strong-field part of the region the deviations of the $L=720$ data from the line are considerably larger than the one-σ_Λ error bars, leading to unacceptably small χ^2 probabilities in a weighted least-squares fit. These deviations may possibly indicate the presence of small but statistically significant corrections to the droplet-theory result. To obtain an acceptable fit for $L=720$ we therefore successively eliminated the data point with the largest value of $|H|$ until the χ^2 probability Q stabilized at a rea-

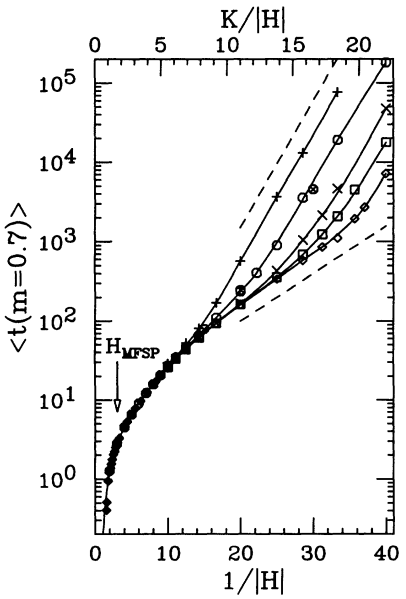

FIG. 2. Mean metastable lifetime for a two-dimensional kinetic Ising model at $T=0.8T_c$, estimated as average first-passage times to $m=0.7$ ($\phi_s\approx0.13$). The simulation was performed by the Metropolis MC algorithm with sequential updates. The lifetimes are given in units of Monte Carlo steps per spin (MCS) and are shown on a logarithmic scale vs $1/|H|$. The symbols indicate data for system sizes $L=64$ (+), 128 (○), 256 (×), 400 (□), and 720 (◊), all obtained with a special-purpose m-TIS2 computer, and $L=128$ (⊗) and 720 (filled diamonds), obtained on heterogeneous workstation clusters. The solid curves are merely guides to the eye. The vertical arrow indicates the inverse field at which droplet theory is expected to break down, $1/H_{\rm MFSP}\approx3$. The L-dependent data in the upper right-hand sector lie in the single-droplet region, the L-independent data in the central portion of the figure lie in the multidroplet region, and the L-independent data in the lower left-hand sector belong to the strong-field region. The dashed line above the data has a slope of 0.36, estimated from the four points for $L=64$ with $1/|H|\geq20$, and the dashed line below the data has 1/3 this slope. The standard deviations in the average lifetimes range from on the order of the symbol size for the weakest fields shown to two orders of magnitude smaller for the strongest fields, and error bars are therefore not shown. See details in Sec. IV.

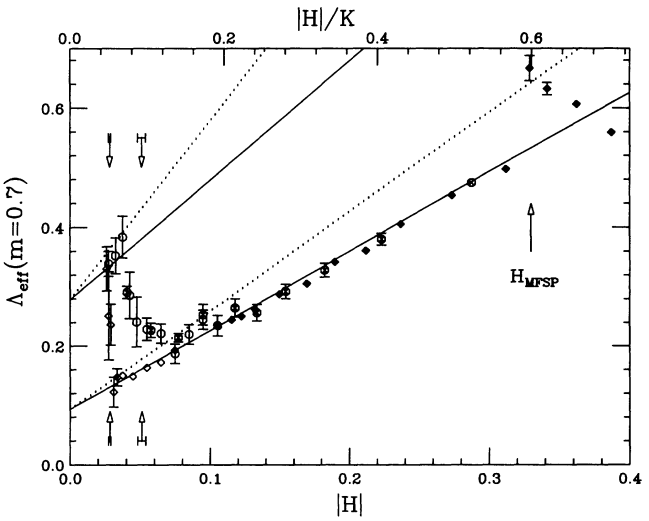

FIG. 3. Finite-difference estimates for the effective slope $\Lambda_{\rm eff}$ from Eq. (21), shown vs $|H|$. The parameters and symbols are the same as in Fig. 2. For clarity only data for $L=128$ (○ and ⊗) and 720 (empty and filled diamonds) are included, and error bars are shown only where larger than the symbol size. The solid straight lines correspond to Eq. (21) with $b+c=2$ and intersect the vertical axis at the exact $\Xi(0.8T_c)$ and $\Xi(0.8T_c)/3$, respectively. The lower solid line gives a good fit to the data in the multidroplet region for both system sizes. Only $L=128$ penetrates fully into the single-droplet region, where the agreement with the theoretical prediction (upper solid line) is also good. The dotted lines, which correspond to $b+c=3$, do not fit the data as well. The crossover between the multi- and single-droplet regions is seen as a jump in $\Lambda_{\rm eff}$. The vertical arrows with horizontal error-bar "feathers" indicate the positions of the estimator $H_{1/2}$ for the crossover field $H_{\rm DSP}$, obtained from Fig. 5(a). The left pair of arrows corresponds to $L=720$ and the right pair to $L=128$. The vertical arrow marked $H_{\rm MFSP}$ marks the L-independent field at which droplet theory is expected to break down. See details in Sec. IV.

sonable value greater than 0.1. The resulting fit, which includes 12 points in the field interval $0.03<|H|<0.15$, gives $b+c=1.95(8)$ and $\Xi(0.8T_c)=0.282(8)$ with $Q=0.41$, consistent with the parameters used to draw the solid straight lines.

Only the smaller system penetrates fully into the single-droplet region in the field range for which data could be obtained with a reasonable amount of computer time. As seen from the figure, the agreement between the $L=128$ MC data and the solid line is also good in the single-droplet region, even though the error bars are larger there than in the multidroplet region.

The dotted straight lines in the figure correspond to Eq. (21) with $b+c=3$, the value expected from the discussion following Eq. (8), and the exact $\Xi(0.8T_c)$. The agreement with the data is far inferior to the solid lines. Since the field-theoretical prediction of $b=1$ has been well confirmed by several numerical methods [39–41,43–46], we believe the disagreement between the predicted and observed values of $b+c$ must be ascribed to c, the exponent giving the field dependence of the kinetic prefactor. (An alternative explanation, that the field dependence of the droplet growth rate $v_0 \sim |H|$ might be wrong, is probably ruled out since this only would affect the fit in the multidroplet region.) We therefore conclude that our numerical results agree well with the predictions of droplet theory, but with $c\approx 1$ instead of $c=2$. We believe the unexpected value of c is an expression of the nonuniversality of the kinetic prefactor and that it is a consequence of the sequential MC update scheme. This view is supported by the simulations with random updates, which we report at the end of this section.

In the strong-field region, droplet theory is not expected to be applicable. For fields beyond $H_{\mathrm{MFSP}}(0.8T_c)\approx 0.3$, Λ_{eff} indeed exhibits pronounced oscillations with H, the first of which can be seen in the right-hand portion of Fig. 3. Further study at these extreme fields is left for future work.

The crossover between the multidroplet and single-droplet regions is clearly seen in Fig. 3 as a jump in Λ_{eff}. However, it is difficult to determine the corresponding dynamic spinodal field H_{DSP} directly from this figure with sufficient accuracy to verify Eq. (17). Instead, we consider the relative standard deviation r, which is shown in Fig. 4 on a logarithmic scale vs $1/|H|$. The error bars in the figure are estimated by standard error-propagation methods as

$$\sigma_r = \frac{r}{\sqrt{2(n-1)}}\left(1+\frac{2(n-1)}{n}r^2\right)^{1/2}.$$

In agreement with our predictions, r crosses over from the behavior described by Eq. (14) for large $|H|$ to $r\approx 1$ for smaller $|H|$. We take as our estimate for H_{DSP} the field $H_{1/2}$ for which $r=0.5$. This field is determined for each value of L from the crossing of a weighted least-squares fit to $\ln r$ in the linear region of Fig. 4 with the horizontal line $r=0.5$. The resulting estimates are shown in Fig. 5(a) as $1/H_{1/2}$ vs L on a logarithmic scale, with error bars estimated from those in Fig. 4 by standard error-propagation methods. The solid curve in Fig. 5(a), which agrees well with the data, represents the crossover condition $L\propto R_0$, where R_0 is given by Eq. (10b) with $b+c=2$ in agreement with the fits in Fig. 3, and with the proportionality constant adjusted to minimize the weighted sum of squares. For reference a dashed line with the asymptotic slope $3/\Xi(0.8T_c)$, expected from Eq. (17), is also included. It was obtained by using the same proportionality constant as in the solid-curve fit and setting the power-law prefactor equal to unity in Eq. (10b). The values of $H_{1/2}$ for $L=128$ and 720 are also indicated by arrows in Fig. 3. The asymptotic L dependence of the lifetime at the DSP, given by Eq. (18), is illustrated in Fig. 5(b). For each L this lifetime was obtained by interpolation between the two closest field values bracketing $H_{1/2}$ for which simulations had been performed, and the uncertainty in the resulting estimate was obtained from those in Figs. 5(a) and 2 by standard error propagation. The numerical results are consistent with the analytical prediction.

The crossover field between the single-droplet and coexistence regions, H_{THSP} of Eq. (20), is not easily observable in our calculation because of the smallness of the numerical factor $(d-1)\hat{\Sigma}(0.8T_c)/(2dk_BTm_s)=0.382\,204\ldots$. Nevertheless, for $L=64$ and cutoff at $m=0.9$ ($\phi_s\approx 0.03$) the resulting prediction is $1/H_{\mathrm{THSP}}\approx 28.5$. As shown in Fig. 6, which corresponds to Fig. 2 except that the cutoff is $m=0.9$, this estimate agrees well with the numerical data. A similar crossover was also observed in Ref. [15]. Except for the behavior for $L=64$ at low fields, and larger uncertainties in general, Fig. 6 is similar to Fig. 2.

One can ask several questions regarding the effects of different local dynamics on the metastable lifetimes. The

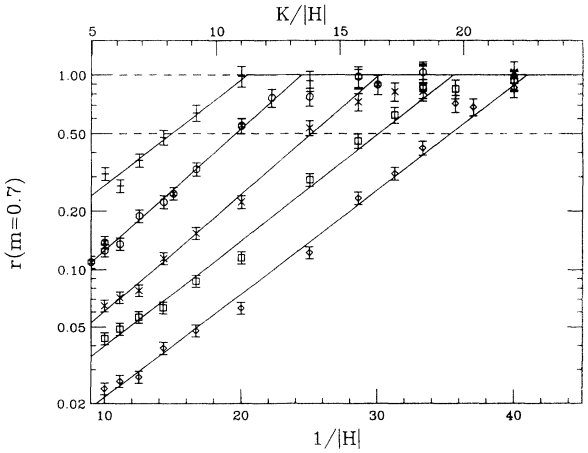

FIG. 4. The relative standard deviation r for $t(m=0.7)$, shown on a logarithmic scale vs $1/|H|$. The parameters and symbols are the same as in Fig. 2. The behavior of r crosses over from the approximate straight line described by Eq. (14) in the multidroplet region to $r\approx 1$ in the single-droplet region. The inclined solid lines are weighted least-squares fits to the data in the region $1/|H|\geq 10$, $r\leq 0.6$. Their average effective slope is 0.13(1), which is intermediate between $\Xi(0.8T_c)$ and $\Xi(0.8T_c)/3$. The estimates $H_{1/2}$ for H_{DSP} are found where these lines cross the horizontal dashed line at $r=0.5$. These estimates are also shown vs L in Fig. 5(a) and are indicated by arrows in Fig. 3. See details in Sec. IV.

difference between the Metropolis dynamics used here and Glauber dynamics should be minor, at least for relatively weak fields [31], and we expect our main conclusions to remain valid for the latter as well. Perhaps more surprisingly, simulations with a modified Swendsen-Wang algorithm [17,20,56] also seem to agree qualitatively with the droplet-theory predictions.

The data presented above were obtained with a sequential-update algorithm. This is fast and well suited to the architecture of the m-TIS2 computer, but it is clearly an unrealistic depiction of any physical dynamics. To estimate the effects of the update scheme we also simulated the L=128 and 720 systems using the same Metropolis MC algorithm as in the sequential-update study, but with updates at randomly chosen sites. This study was conducted entirely on heterogeneous workstation clusters.

The most noticeable difference between the two update schemes is that it takes a considerably larger number of MCS to reach a given cutoff magnetization with random updates than with sequential ones. This effect and its nontrivial field dependence are illustrated in Fig. 7, which shows the ratio between the random and sequential lifetimes $\langle t_R(m{=}0.7)\rangle/\langle t_S(m{=}0.7)\rangle$ for L=128 and 720. Since the universal part of the field dependence must cancel in this ratio, its dominant field dependence is obtained from Eqs. (10a) and (16) as

$$\frac{\langle t_R(\phi_s)\rangle}{\langle t_S(\phi_s)\rangle} \propto \begin{cases} |H|^{-\frac{c_R-c_S}{d+1}} & \text{in the multidroplet region} \\ |H|^{-(c_R-c_S)} & \text{in the single-droplet region,} \end{cases} \tag{22}$$

with proportionality constants that depend only on T. Here c_R and c_S are the nonuniversal kinetic-prefactor exponents for random and sequential updates, respectively. This pure power-law behavior is only seen for L=720 in the weak-field portion of the multidroplet region, indicating that additional nonuniversal effects distinguish between the behaviors of the two update schemes for stronger fields. Following the procedure described in the discussion of Fig. 3, we obtained a weighted least-squares fit to the L=720 data, including ten points in the field interval $0.028 \le |H| \le 0.09$. This fit, which is shown as a solid line in the figure, yields $(c_R - c_S) = 1.24(3)$ with Q=0.44. In view of the very short fitting interval, this estimate should only be taken as an indication that the difference between the two values of c is probably on the order of unity.

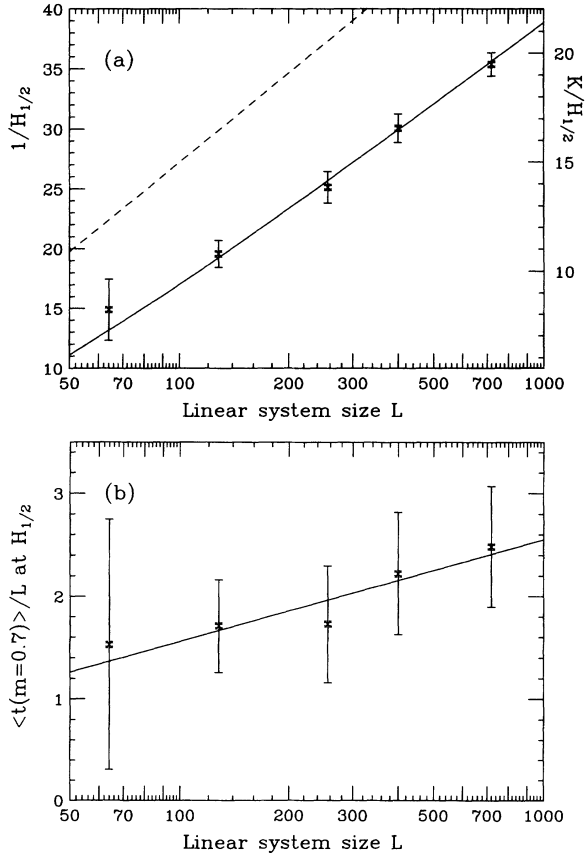

FIG. 5. Inverse field and mean lifetime at the DSP. (a) The estimates $1/H_{1/2}$ for $1/H_{DSP}$ as obtained from Fig. 4, shown vs L on a logarithmic scale. The solid curve corresponds to $L \propto R_0$ with $b+c=2$ in Eq. (10b) and with the proportionality constant adjusted to minimize the weighted sum of squares. The dashed line indicates the asymptotic slope $3/\Xi(0.8T_c)$. (b) The average lifetimes at $1/H_{1/2}$. The solid straight line is a weighted least-squares fit. The figure supports the asymptotic behavior given in Eq. (18), $\langle t \text{ at } H_{DSP}\rangle \propto L \ln L$. See details in Sec. IV.

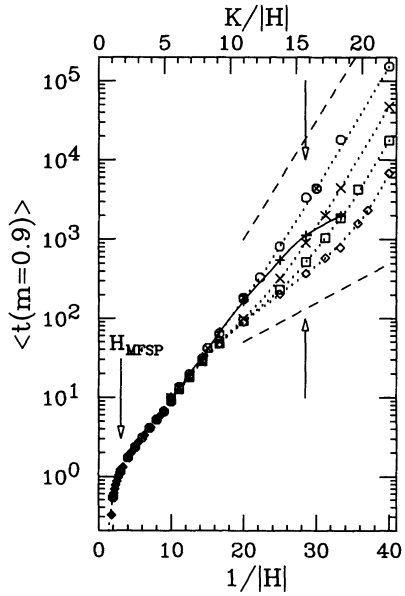

FIG. 6. Mean metastable lifetimes at $T=0.8T_c$, estimated as average first-passage times to m=0.9 ($\phi_s \approx 0.03$). The parameters and symbols are otherwise the same as in Fig. 2. Except for somewhat larger uncertainties and the behavior for L=64 at low fields, this figure is similar to Fig. 2. The guide-to-the-eye curves are dotted, except for L=64, which has been drawn solid to emphasize the behavior for this smallest system. It crosses over between the single-cluster and coexistence regions at a ϕ_s-dependent $H_{THSP} \approx 28.5$ (marked by the opposing arrows), as discussed in Sec. IV.

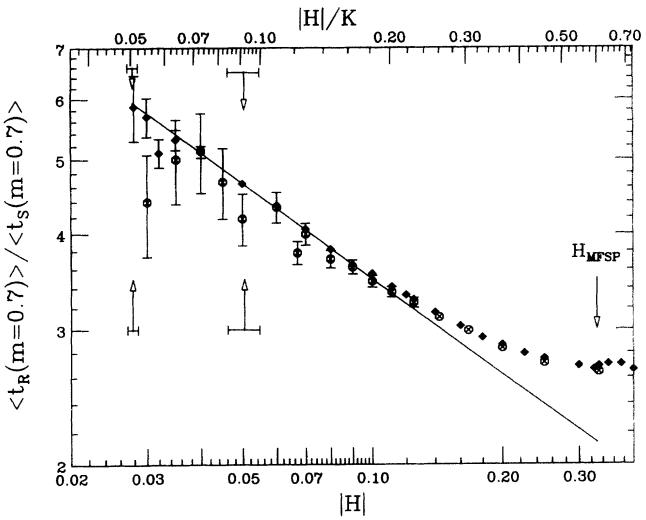

FIG. 7. The ratio $\langle t_R\rangle/\langle t_S\rangle$ between the mean lifetimes obtained with random and sequential MC updates for L=128 and 720. The symbols and parameters are the same as in Figs. 3 and 8. The two pairs of opposing arrows with horizontal error-bar "feathers" mark $H_{1/2}$ for the two system sizes. The solid straight line in this log-log plot is a weighted least-squares fit to Eq. (22) in the weak-field part of the multidroplet region for L=720. See details in Sec. IV.

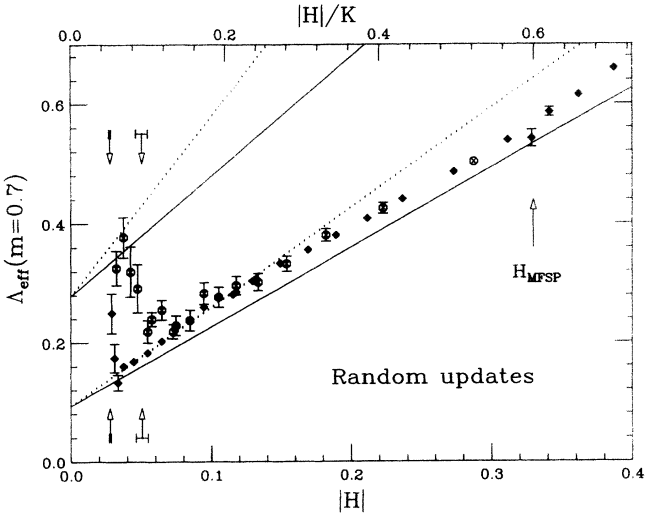

FIG. 8. Finite-difference estimates for the effective slope Λ_{eff} from Eq. (21) for random MC updates with L=128 and 720, shown vs $|H|$. The figure is analogous to Fig. 3, and the symbols and parameters are the same as in that figure. The behavior is similar to the sequential-update case, except that the prefactor exponent $b+c\approx 3$ and the field interval in which Λ_{eff} seems to follow a linear approach to the exact $\Xi/3$ is narrower than in Fig. 3. See details in Sec. IV.

A somewhat puzzling feature in Fig. 7 is the falloff of the ratio for L=128 in the single-droplet region. We believe this may be due to the proximity of the THSP for this relatively small system size.

In Fig. 8, which corresponds to and should be compared with Fig. 3, we show the effective slope Λ_{eff} from Eq. (21) for the random-update case. The estimated $H_{1/2}$ for both L=128 and 720 (indicated by opposing arrows in the figure) agree to within the statistical error with the estimates for sequential updates. In the weak-field portion of the multidroplet region the effective slopes follow the lower dotted line, which has the same meaning as in Fig. 3. Two major differences from the sequential-update case are apparent. First, the field interval in which Λ_{eff} seems to follow a linear approach to the exact $\Xi(0.8T_c)/3$ is narrower, as one would expect from the behavior of the lifetime ratios shown in Fig. 7. Second, the fact that the effective slopes cluster around the *dotted* line indicates that the nonuniversal prefactor exponent c is close to 2, as expected for dynamics that can be described by a Fokker-Planck equation [24–26]. Following the procedure described above, we obtained a weighted least-squares fit to the L=720 data, including ten points in the interval $0.03<|H|<0.11$. The resulting parameter estimates were $\Xi(0.8T_c)=0.260(11)$ and $c=2.41(15)$ with $Q=0.22$. In view of the short fitting interval we consider that this estimate is consistent with the expected exact values. For $|H|>0.11$ the deviation of Λ_{eff} from the dotted straight line takes the form of a smooth, slow oscillation whose amplitude is much larger than the statistical errors.

In summary, our results indicate that the main difference in the nonuniversal part of the field dependence of the metastable lifetimes between the sequential and random update schemes lies in the kinetic-prefactor exponent c. For sequential updates we find $c\approx 1$, whereas for random updates $c\approx 2$, in agreement with the theoretical expectation $c=2$. In addition to the difference in c for weak fields, the quantitative differences between the lifetimes in the two update schemes become progressively larger with increasing $|H|$.

V. DISCUSSION

We have demonstrated that the metastable lifetimes for impurity-free kinetic Ising models with nearest-neighbor interactions and local dynamics, in weak to moderate unfavorable applied fields, exhibit system-size and field dependences that can be explained by a field-theoretical droplet model of homogeneous nucleation [23–26]. The most significant determining factor for the lifetime is the free energy of a critical droplet of the stable phase, which in a wide field interval leads to an exponential dependence on the inverse applied field. This free energy is independent of the details of the local dynamics, and it can be accurately calculated by combining a Wulff construction with the exact zero-field equilibrium surface tension.

Our numerical estimates for the lifetimes, based on Monte Carlo simulations in two dimensions, are in excellent agreement with the droplet model. This agreement includes both the aforementioned exponential dependence on the inverse field and multiplicative power-law prefactors. There are two independent contributions to these prefactors: a universal exponent b, equal to unity

for d=2, and a nonuniversal exponent c, which depends on the details of the dynamics. Our results indicate that with MC updates at randomly chosen sites, c is close to 2, which is the exact result for dynamics described by a Fokker-Planck equation [24,25]. With sequential updates we found $c \approx 1$. It is tempting to conjecture that the exact value in this case is unity, but at present we have no theoretical arguments to substantiate this suggestion. For stronger fields we found additional, dynamics-dependent deviations from the droplet-theory predictions for Λ_{eff}.

We have identified four different field regions, in which the decay proceeds through different excitations. In order of increasingly strong unfavorable field $|H|$, these were the coexistence region, characterized by subcritical fluctuations on the scale of the system volume; the single-droplet region, characterized by decay via a single critical droplet; the multidroplet region, characterized by decay via a finite density of droplets; and the strong-field region, in which the droplet picture is inappropriate. The crossover fields between these regions

$$[H_{\text{THSP}} \sim L^{-1}] < [H_{\text{DSP}} \sim (\ln L)^{-\frac{1}{d-1}}] < [H_{\text{MFSP}} \sim L^{0}] \tag{23}$$

are accurately predicted by droplet theory. The different regions and crossover fields are illustrated in Fig. 1. We believe the slow, logarithmic vanishing with system size of the dynamic spinodal field H_{DSP}, which separates the single-droplet and multidroplet regions, is of particular significance. This convergence is so slow, especially in three and higher dimensions, that systems that are rightfully considered macroscopic in terms of their equilibrium properties may nevertheless possess a measurable single-droplet region in which the metastable state is exceedingly long lived on the average.

Noted added in proof. After this paper was accepted for publication we became aware of two recent theoretical studies which consider finite-size effects and the interplay between nucleation and growth in metastable decay, as applied to the switching behavior of ferroelectric films [H. M. Duiker and P. D. Beale, Phys. Rev. B **41**, 490 (1990); H. Orihara and Y. Ishibashi, J. Phys. Soc. Jpn. **61**, 1919 (1992)]. The paper by Duiker and Beale also contains Monte Carlo results for a two-dimensional kinetic Ising model.

ACKNOWLEDGMENTS

We gratefully acknowledge discussions with J. Lee, M. A. Novotny, B. M. Gorman, and C. C. A. Günther, and helpful comments on an earlier version of this paper by D. Stauffer. The numerical values for $\widehat{\Sigma}(0.8T_c)$ and $H_{\text{MFSP}}(0.8T_c)$ were provided by C. C. A. Günther. P.A.R. greatly enjoyed the kind hospitality at Kyoto University. This study was supported by a Grant-In-Aid for Scientific Research on Priority Area "Computational Physics as a New Frontier in Condensed Matter Research" from the Ministry of Education, Science, and Culture of Japan, and by National Science Foundation Grants No. DMR-9013107 and DMR-9315969. It was also supported by Florida State University through the Supercomputer Computations Research Institute (Department of Energy Contract No. DE-FC05-85ER25000) and the Center for Materials Research and Technology.

[1] J. E. McDonald, Am. J. Phys. **30**, 870 (1962); **31**, 31 (1963). Reprinted in Ref. [2].
[2] F. F. Abraham, *Homogeneous Nucleation Theory* (Academic, New York, 1974).
[3] R. J. Speedy and C. A. Angell, J. Chem. Phys. **65**, 851 (1976); P. H. Poole, F. Sciortino, U. Essmann, and H. E. Stanley, Nature **360**, 324 (1992); Y. Viisanen, R. Strey, and H. Reiss, J. Chem. Phys. **99**, 4680 (1993).
[4] See, e.g., M. Gleiser and E. Kolb, Int. J. Mod. Phys. C **3**, 773 (1992); J. Kripfganz, *ibid.* **3**, 783 (1992); W. Buchmüller and T. Helbig, *ibid.* **3**, 799 (1992).
[5] See, e.g., K. Kajantie, Int. J. Mod. Phys. C **3**, 921 (1992); M. Hackel, M. Faber, H. Markum, and M. Müller, *ibid.* **3**, 961 (1992).
[6] L. S. Schulman, in *Finite-Size Scaling and Numerical Simulation of Statistical Systems*, edited by V. Privman (World Scientific, Singapore, 1990).
[7] O. Penrose and J. L. Lebowitz, J. Stat. Phys. **3**, 211 (1971); in *Fluctuation Phenomena*, edited by E. W. Montroll and J. L. Lebowitz (North-Holland, Amsterdam, 1979), Chap. 5, p. 293.
[8] References to work on long-range models can be found in B. M. Gorman, P. A. Rikvold, and M. A. Novotny, Phys. Rev. E **49**, 2711 (1994); T. Fiig, B. M. Gorman, P. A. Rikvold, and M. A. Novotny (unpublished).
[9] M. E. Fisher, in *Proceedings of the Gibbs Symposium, Yale University, 1989*, edited by G. D. Mostow and D. G. Caldi (American Mathematical Society, Providence, RI, 1990).
[10] E. Stoll and T. Schneider, Phys. Rev. A **6**, 429 (1972).
[11] K. Binder, Phys. Rev. B **8**, 3419 (1973).
[12] K. Binder and E. Stoll, Phys. Rev. Lett. **31**, 47 (1973).
[13] K. Binder and H. Müller-Krumbhaar, Phys. Rev. B **9**, 2328 (1974).
[14] E. P. Stoll and T. Schneider, Physica **86-88B**, 1419 (1977).
[15] R. J. McCraw and L. S. Schulman, J. Stat. Phys. **18**, 293 (1978).
[16] W. Paul and D. W. Heermann, Europhys. Lett. **6**, 701 (1988).
[17] T. S. Ray and P. Tamayo, J. Stat. Phys. **60**, 851 (1990).
[18] A review of early MC work on metastable decay is given by K. Binder, in *Phase Transitions and Critical Phenomena*, edited by C. Domb and M. Green (Academic, London, 1976), Vol. 5B.
[19] D. Stauffer, A. Coniglio, and D. W. Heermann, Phys. Rev. Lett. **49**, 1299 (1982).
[20] T. S. Ray and J.-S. Wang, Physica A **167**, 580 (1990).
[21] D. Stauffer, Int. J. Mod. Phys. C **3**, 1059 (1992).
[22] M. E. Fisher, Physics **3**, 255 (1967).

[23] J. S. Langer, Ann. Phys. (N.Y.) **41**, 108 (1967).
[24] J. S. Langer, Phys. Rev. Lett. **21**, 973 (1968).
[25] J. S. Langer, Ann. Phys. (N.Y.) **54**, 258 (1969).
[26] N. J. Günther, D. A. Nicole, and D. J. Wallace, J. Phys. A **13**, 1755 (1980).
[27] J. D. Gunton and M. Droz, *Introduction to the Theory of Metastable and Unstable States* (Springer, Berlin, 1983).
[28] O. Penrose, J. Stat. Phys. (to be published).
[29] H. Tomita and S. Miyashita, Phys. Rev. B **46**, 8886 (1992).
[30] H. Tomita and S. Miyashita, in *Computational Approaches in Condensed-Matter Physics*, edited by S. Miyashita, M. Imada, and H. Takayama (Springer, Berlin, 1992), p. 278.
[31] H. Müller-Krumbhaar and K. Binder, J. Stat. Phys. **8**, 1 (1973).
[32] K. K. Mon and D. Jasnow, Phys. Rev. Lett. **59**, 2983 (1987).
[33] C. N. Yang, Phys. Rev. **85**, 808 (1952).
[34] R. K. P. Zia and J. E. Avron, Phys. Rev. B **25**, 2042 (1982).
[35] N. Ito, M. Taiji, and M. Suzuki, J. Phys. Soc. Jpn. **56**, 4218 (1987).
[36] N. Ito, M. Taiji, and M. Suzuki, in *Computational Approaches in Condensed-Matter Physics* (Ref. [30]), p. 297.
[37] C. Rottman and M. Wortis, Phys. Rev. B **24**, 6274 (1981).
[38] J. E. Avron, H. van Beijeren, L. S. Schulman, and R. K. P. Zia, J. Phys. A **15**, L81 (1982).
[39] C. K. Harris, J. Phys. A **17**, L143 (1984).
[40] C. C. A. Günther, P. A. Rikvold, and M. A. Novotny, Phys. Rev. Lett. **71**, 3898 (1993).
[41] C. C. A. Günther, P. A. Rikvold, and M. A. Novotny (unpublished).
[42] Our quantity $\widehat{\Sigma}(T)$ is identical to $dW^{1/d}$ in Eq. (3) of Ref. [34].
[43] G. Jacucci, A. Perini, and G. Martin, J. Phys. A **16**, 369 (1983).
[44] A. Perini, G. Jacucci, and G. Martin, Phys. Rev. B **29**, 2689 (1984); Surf. Sci. **144**, 53 (1984).
[45] M. J. Lowe and D. J. Wallace, J. Phys. A **13**, L381 (1980).
[46] D. J. Wallace, in *Phase Transitions*, Proceedings of a Summer Institute, Cargèse, Corsica, 1980, edited by M. Levy, J. C. Le Guillou, and J. Zinn-Justin (Plenum, New York, 1982), p. 423.
[47] See, e.g, E. Brener, K. Kassner, H. Müller-Krumbhaar, and D. Temkin, Int. J. Mod. Phys. C **3**, 825 (1992).
[48] S. M. Allen and J. W. Cahn, Acta Metall. **27**, 1085 (1979).
[49] K. Sekimoto, Physica **135A**, 328 (1986); Int. J. Mod. Phys. B **5**, 1843 (1991).
[50] A. N. Kolmogorov, Bull. Acad. Sci. USSR, Phys. Ser. **1**, 355 (1937).
[51] W. A. Johnson and P. A. Mehl, Trans. Am. Inst. Min. Metall. Eng. **135**, 416 (1939).
[52] M. Avrami, J. Chem. Phys. **7**, 1103 (1939); **8**, 212 (1940); **9**, 177 (1941).
[53] E. Jordão Neves and R. Schonmann, Commun. Math. Phys. **137**, 209 (1991).
[54] R. Schonmann, Commun. Math. Phys. **147**, 231 (1992).
[55] H. Tomita and S. Miyashita (unpublished).
[56] R. Swendsen and J.-S. Wang, Phys. Rev. Lett. **58**, 86 (1987).